Procedia Computer Science

Volume 51, 2015, Pages 934–943

ICCS 2015 International Conference On Computational Science

Coupling Navier-Stokes and Cahn-Hilliard equations in a two-dimensional annular flow configuration

Philippe Vignal[1], Adel Sarmiento[2], Adriano M.A. Côrtes[3], Lisandro Dalcin[4], and Victor.M. Calo[5]

[1] Center for Numerical Porous Media (NumPor),
Materials Science and Engineering (MSE),
King Abdullah University of Science and Technology, Thuwal, Saudi Arabia
philippe.vignal@kaust.edu.sa

[2] Center for Numerical Porous Media (NumPor),
Applied Mathematics and Computational Science (AMCS),
King Abdullah University of Science and Technology, Thuwal, Saudi Arabia
adel.sarmientorodriguez@kaust.edu.sa

[3] Center for Numerical Porous Media (NumPor),
King Abdullah University of Science and Technology, Thuwal, Saudi Arabia
adriano.cortes@kaust.edu.sa

[4] Consejo Nacional de Investigaciones Científicas y Técnicas, Santa Fe, Argentina
Center for Numerical Porous Media (NumPor),
King Abdullah University of Science and Technology, Thuwal, Saudi Arabia
dalcinl@gmail.com

[5] Center for Numerical Porous Media (NumPor),
Applied Mathematics and Computational Science (AMCS),
Earth Sciences and Engineering (ErSE),
King Abdullah University of Science and Technology, Thuwal, Saudi Arabia
victor.calo@kaust.edu.sa

Abstract

In this work, we present a novel isogeometric analysis discretization for the Navier-Stokes-Cahn-Hilliard equation, which uses divergence-conforming spaces. Basis functions generated with this method can have higher-order continuity, and allow to directly discretize the higher-order operators present in the equation. The discretization is implemented in PetIGA-MF, a high-performance framework for discrete differential forms. We present solutions in a two-dimensional annulus, and model spinodal decomposition under shear flow.

Keywords: Phase-field modeling, Navier-Stokes equation, high-order partial differential equation, isogeometric analysis, divergence-conforming spaces

 Selection and peer-review under responsibility of the Scientific Programme Committee of ICCS 2015

doi:10.1016/j.procs.2015.05.228

1 Introduction

When a homogeneous mixture is quenched into a metastable or spinodal regime, interesting and complex patterns can emerge during the phase-separation of the fluids involved [16]. Understanding the morphology and the kinetics ruling the phase-transition process requires answering thermodynamical and hydrodynamical questions, making research on this topic relevant from a fundamental point of view. Making matters even more relevant, is the fact that these patterns can be influenced by the presence of external fields. These fields can be of either dissipative or non-dissipative nature [32], and can add to the system new characteristic length and time scales [37]. These problems are interesting because the steady state after quenching is in non-equilibrium, driven by the external fields as opposed to that of normal spinodal decomposition. In the case of a binary fluid mixture under shear flow [29], it has been observed experimentally [23] that the shear rate introduces a new time scale. The competition between the phase separation process, due to the thermodynamical instability [6, 30], and the breakup mechanism by shear, reaches a steady state that gives rise to anisotropic domain structures [25]. At steady state, the fluid mixture separates into two distinct phases and forms a banded structure stretched along the flow domain [16, 23, 28].

To describe the spinodal decomposition of a binary fluid, the Cahn-Hilliard equation was proposed [6, 7]. In it, the free energy of the system is expressed in terms of a phase-field variable, whose physical meaning is related to concentration, as well as its derivatives with respect to the phase-field, which account for interfacial energy or surface tension. The Cahn-Hilliard equation is a stiff, nonlinear, fourth-order partial differential equation, that describes the dissipation process of this free energy, often referred to as the Ginzburg-Landau free energy [21]. The process is driven by a competition between the minimization of a chemical free energy, usually represented by either a polynomial or a logarithmic function [21], and the minimization of the interfacial energy. The minimization of the chemical free energy, described as a double well potential, leads the phase-field to binodal points, whereas the minimization of the interfacial energy resists the growth of the interfacial area. Including the flow field within this setting can be done by coupling the Cahn-Hilliard equation with the Navier-Stokes system.

Numerical experiments to simulate spinodal decomposition under uniform shear flow have been performed [20, 28, 35] but research into this topic is still ongoing. The complicated nature of the equation warrants consideration of advanced numerical techniques, used on high-performance platforms, to get steady-state solutions while overcoming the limitations of more traditional numerical methods [27]. This is the motivation and the focus of this work, where a novel discretization of the equation is proposed, which is compatible with the mathematical structure of the equation being solved. The discretization is based on isogeometric analysis [14], with which globally $\mathcal{C}^k$-continuous basis functions, where $k \geqslant 0$, can be produced while avoiding the use of mixed forms [15, 33]. This is advantageous when dealing with higher-order partial differential equations, as shown in [21, 22, 34]. Borrowing the theory of isogeometric differential forms, it is possible to satisfy the inf-sup stability condition of the discrete velocity-pressure pair. Using the corresponding divergence-conforming and integral-conforming spaces for the velocity and pressure fields, respectively, guarantees the physical incompressibility condition exactly at the discrete level [4]. The implementation was done using PetIGA-MF, a multi-field high-performance implementation of divergence-conforming B-splines [31] which is built on top of PetIGA [8, 13].

The work is organized as follows. In section 2 we review the Navier-Stokes-Cahn-Hilliard model. Section 3 covers the discretization used for the equation, while in section 4 we discuss preliminary results obtained. We conclude in section 5 and future work is covered in section 6.

2 Navier-Stokes-Cahn-Hilliard system

Let $\Omega_T \in \mathbb{R}^d$ be an arbitrary open domain, where $d = 2$ or 3. The boundary of Ω_T is denoted Γ, while the outward directed unit vector normal to Γ is denoted as $\mathbf{n}$. A binary mixture is contained in Ω_T, with the phase-field denoted by ϕ, which effectively represents the concentration of one of the components present in the system. Given the focus of this work, we forego the derivation of the Cahn-Hilliard equation that can be found in [21, 30]. The Ginzburg-Landau free energy used in this paper, denoted by $\mathcal{F}[\phi]$, is given by [21]

$$\begin{aligned}\mathcal{F}[\phi] &= \int_{\Omega_T} f(\phi, \nabla\phi)\ \mathrm{d}\Omega_T, \\ &= \int_{\Omega_T} \Psi(\phi) + \frac{\gamma}{2}|\nabla\phi|^2\ \mathrm{d}\Omega_T, \end{aligned} \tag{1}$$

where $\Psi(\phi) = 1/(2\theta)\big(\phi\log\phi + (1-\phi)\log(1-\phi)\big) + \phi(1-\phi)$, is the bulk free energy density that includes entropic effects, and $\gamma/2|\nabla\phi|^2$ is the internal energy contribution to the free energy. As previously mentioned, the latter term is used to model interfacial effects. The parameter γ is a positive constant related to the interface thickness. This term is a strictly positive quantity, which means that if it increases, so will the free energy. This is the reason behind the standard steady state solutions for the Cahn-Hilliard equation found in the literature (i.e., bubbles, spheres, or cylinders [21, 36]) when simulating spinodal decomposition of a binary mixture with periodic boundary conditions, as these surfaces minimise the interfacial area. The variational derivative of equation (1) with respect to ϕ, is the Euler-Lagrange equation [30]

$$\frac{\delta\mathcal{F}}{\delta\phi} = \frac{\delta f}{\delta\phi} - \nabla\cdot\frac{\delta f}{\delta\nabla\phi} \tag{2}$$

which, when considering this term as a flux as well as the fact that there is conservation of mass, leads to the Cahn-Hilliard equation

$$\phi_t = \nabla\cdot\left(M(\phi)\nabla\left(\Psi'(\phi) - \gamma\Delta\phi\right)\right), \tag{3}$$

where $\phi_t = \dfrac{\partial\phi}{\partial t}$, the mobility function M is defined as $M(\phi) = \phi(1-\phi)$, and $\Psi'(\phi)$ represents the chemical potential given by

$$\Psi'(\phi) = \frac{1}{2\theta}\log\left(\frac{\phi}{1-\phi}\right) + 1 - 2\phi.$$

The parameter θ represents the ratio between the critical and the absolute temperature, and is assigned a value of $3/2$ so as to lie inside the spinodal regime. The Navier-Stokes-Cahn-Hilliard equation is then obtained by coupling the Cahn-Hilliard equation (3) with the conservation of linear momentum equation [2], such that [20]

$$\mathbf{u}_t + \nabla\cdot(\mathbf{u}\otimes\mathbf{u}) - \nabla\cdot\boldsymbol{\sigma}(\mathbf{u}, p) + \nabla p + \lambda\nabla\cdot(\nabla\phi\otimes\nabla\phi) = \mathbf{f} \quad \text{in} \quad \Omega_T, \tag{4}$$

$$\phi_t + \nabla\cdot(\phi\mathbf{u}) - \nabla\cdot\left(M_c\nabla\left(\Psi'(\phi) - \gamma\Delta\phi\right)\right) = 0 \quad \text{in} \quad \Omega_T, \tag{5}$$

$$\nabla\cdot\mathbf{u} = 0 \quad \text{in} \quad \Omega_T \tag{6}$$

for two immiscible and incompressible fluids with comparable densities and kinematic viscosities ν (assumed to be all equal to one), where $\mathbf{u}(x,t) \in \mathbb{R}^d$ and the scalar $p(x,t) \in \mathbb{R}$ denote the

velocity and the pressure of the fluid mixture at the space time point (x, t), respectively. The phase-field ϕ assumes distinct values in the bulk phases away from the interfacial region, over which ϕ varies smoothly. The constants $\lambda = 0.1$ and $\gamma = 9.54 \cdot 10^{-6}$ represent the surface tension coefficient, and the capillary width (i.e., width of the interfacial layer), respectively. The vector $\mathbf{f}$ defines a constant external forcing.

The momentum conservation equation (4) includes the advective term $\nabla \cdot (\mathbf{u} \otimes \mathbf{u})$, which represents the transport of momentum, as well as the dissipative terms coming from the Cauchy stress tensor, given by

$$\boldsymbol{\sigma}(\mathbf{u}, p) = -p\mathbf{I} + 2\nu\nabla^s\mathbf{u}, \tag{7}$$

where $\nabla^s\mathbf{u}$ is the symmetric gradient of the velocity, $\mathbf{I}$ is the identity matrix, and the surface stress tensor $(\nabla\phi \otimes \nabla\phi)$, also known as capillary tensor [1]. This tensor can be seen as a generator of momentum related to the interface of the phase-field. In the case of incompressible fluids, equation (6) expresses mass conservation in the system. The model is subject to the following initial and boundary conditions

$$\mathbf{u}(., 0) = \mathbf{u}_0(.) \quad \text{in} \quad \Omega_T, \tag{8}$$

$$\phi(., 0) = \phi_0(.) \quad \text{in} \quad \Omega_T, \tag{9}$$

$$\mathbf{u} \cdot \mathbf{n} = 0 \quad \text{on} \quad \partial\Omega_T := \partial\Omega \times (0, T[, \tag{10}$$

$$\frac{\partial\phi}{\partial\mathbf{n}} = \frac{\partial}{\partial\mathbf{n}}\left(\Psi'(\phi) + \gamma\Delta\phi\right) = 0 \quad \text{on} \quad \partial\Omega_T := \partial\Omega_T \times (0, T[. \tag{11}$$

3 Discretization

The model is implemented in PetIGA-MF [31], a framework for high performance computing based on PetIGA [8], that provides structure-preserving discretizations based on discrete differential forms [4], using isogeometric analysis [14]. This method has been shown to possess advantages over standard finite element methods [24], and allows for an easier discretization of high-order partial differential equations, as shown in [8, 14, 17, 21, 31]. This nonetheless comes at a cost, as the linear systems are harder to solve [9, 10, 11], which justifies the use and development of libraries such as PetIGA [8, 13] and PetIGA-MF [31], which allow the use of different discretization spaces for each variable. In this work, given the properties of the Navier-Stokes-Cahn-Hilliard system, we use divergence-, integral-, and H_1-conforming spaces to discretize the velocity, pressure, and phase-field, respectively.

The structure-preserving spaces used in PetIGA-MF are based on the discrete de Rham commuting diagram, defined in the parametric domain as an exact sequence of differential operators [4]. When a pair of discrete spaces satisfy a step of the sequence, they are said to be conformal to the corresponding differential operator, such as gradient-, curl-, divergence-, and integral-conforming spaces. The curl-conforming pair of spaces was first used to satisfy the stability condition of the Maxwell equations [5], and later the divergence-conforming pair was successfully used to model incompressible viscous flow models such as in Stokes and Navier-Stokes equations [3, 12, 18, 19].

The pair of divergence- and integral-conforming spaces, used for velocity and pressure, satisfy the inf-sup stability condition by construction, and guarantee point-wise divergence-free solutions [4], allowing us to model the phase-field conservation equation in an accurate manner. For the sake of simplicity, the phase-field variable is discretized using an H_1-conforming space with the same polynomial order and inter-element continuity as the pressure, whose space is

more regular than minimally needed. The spaces are defined in the $2D$ parametric domain as

Velocity	Divergence-conforming	$\mathcal{S}_{2,1}^{3,2} \times \mathcal{S}_{1,2}^{2,3}$,
Pressure	Integral-conforming	$\mathcal{S}_{1,1}^{2,2}$,
Phase-field	H_1-conforming	$\mathcal{S}_{1,1}^{2,2}$,

where $\mathcal{S}_{\beta_x,\beta_y}^{\alpha_x,\alpha_y}$ is a two-dimensional B-spline function, generated by a tensor product between two one-dimensional B-splines, $\mathcal{S}_{\beta_x}^{\alpha_x}$ and $\mathcal{S}_{\beta_y}^{\alpha_y}$. Here, α_i represents the polynomial order, and β_i stands for the inter-element continuity of the function along the ith axis.

To preserve the divergence-, integral-, and H_1-conforming structure built in the parametric domain, when mapping to the physical domain, each of these spaces has a different structure-preserving mapping to satisfy the exact sequence of the de Rham diagram, which are defined as

Divergence-conforming	$\mathbf{u} = \det(D\mathbf{F})\,(D\mathbf{F})^{-1}\,(\mathbf{u} \circ \mathbf{F})$,	$\mathbf{u} \in \mathbf{H}(\mathrm{div}; \Omega_T)$
Integral-conforming	$p = \det(D\mathbf{F})\,(p \circ \mathbf{F})$,	$p \in L^2(\Omega_T)$
H_1-conforming	$\phi = \phi \circ \mathbf{F}$,	$\phi \in H_1(\Omega_T)$

where the geometric mapping $\mathbf{F}$ maps the reference domain $\widehat{\Omega}$ into the physical domain Ω (Figure 1), and $D\mathbf{F}$ represents the gradient of the geometric mapping. This choice of discretization satisfies the mass conservation equation exactly, providing a point-wise discrete divergence-free velocity field. The conservation of mass in the phase-field equation is given by the divergence of the particle and internal energy flux [30], and by the coupling with the divergence-free velocity in the advective term.

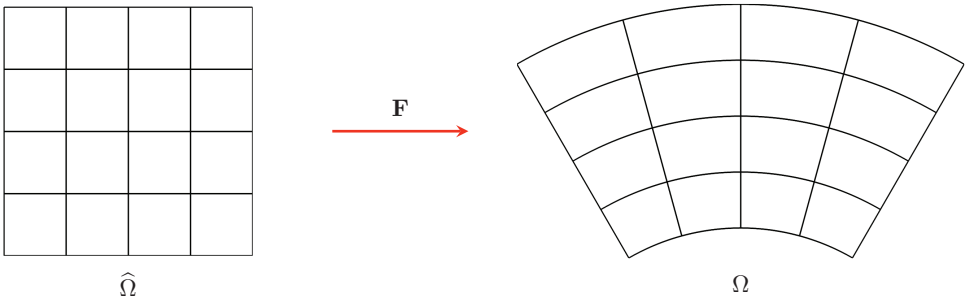

Figure 1: Geometric mapping $\mathbf{F}$ used to map the unitary square into the physical domain.

3.1 Model problem

The formulation is tested on a sixth of an annular section with an inner radius of $r_{in} = 1$ and an outer radius of $r_{out} = 2$. This domain is taken from [28], where it is used together with the advective Cahn-Hilliard equation. The initial condition for the velocity corresponds to that of the steady annular Couette flow, and is shown in Figure 2a. It is defined as

$$\mathbf{u}_0 = \begin{bmatrix} (Ar + \frac{B}{r})\sin(\theta) \\ (Ar + \frac{B}{r})\cos(\theta) \end{bmatrix},$$

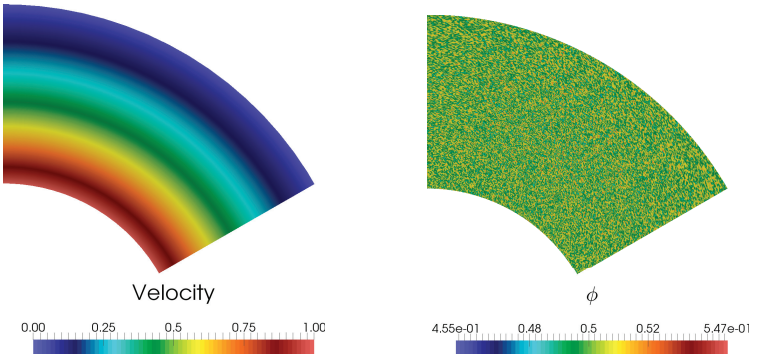

(a) Velocity (b) Phase-field

Figure 2: Initial condition for the velocity field as annular Couette flow, and random initial condition for the phase-field.

where r and θ correspond to the polar coordinates, and

$$A = -\frac{U\,\delta^2}{r_{in}(1-\delta^2)}, \quad B = \frac{U\,r_{in}}{(1-\delta^2)}, \quad \delta = \frac{r_{in}}{r_{out}},$$

with $U = 1$ the imposed tangential velocity at r_{in}, and the tangential velocity equal to zero at r_{out}. The phase-field variable ϕ varies between 0 and 1, and its initial condition ϕ_0 is given by a random function δ_ϕ with normal distribution

$$\phi_0 = \overline{\phi} + \delta_\phi, \tag{12}$$

where $\overline{\phi} = 0.5$ is the average value of ϕ, and $\delta_\phi \in [-0.05, 0.05]$. The initial condition is shown in Figure 2b. Periodic boundary conditions were imposed on the angular axis of the annulus for all the variables. With regards to the temporal discretization, we use the implicit, second-order accurate generalized-α method [26].

4 Numerical examples

We present the solution for the phase-field (Figures 3 to 5) obtained using three meshes having 64^2, 128^2, and 256^2 elements, respectively. Results are shown at several time steps to illustrate the effect of the shear flow over the phase-field distribution, and the effect of the surface tension induced by the phase-field over the velocity field.

Different phenomena are present on the results found, each of them occurring at a different time scale. Phase separation initially takes place at a very high speed, with the simulation requiring a time size on the the order of 10^{-10}. During this process, the first step involves the formation of several small bubbles that start growing and merging. The effect of advection over the phase-field is not noticeable given the small time scale. Once the total time of the simulation is on the order of 10^{-5}, the phases start to coarsen and the effects of advection are noticeable. The flow stretches the bubbles, which then merge together. These effects are mostly seen close to the inner radius, where the velocity is highest. This causes a coarsening of the phase-field, initially toward the inner wall, and gradually reaching the outer wall. This effect

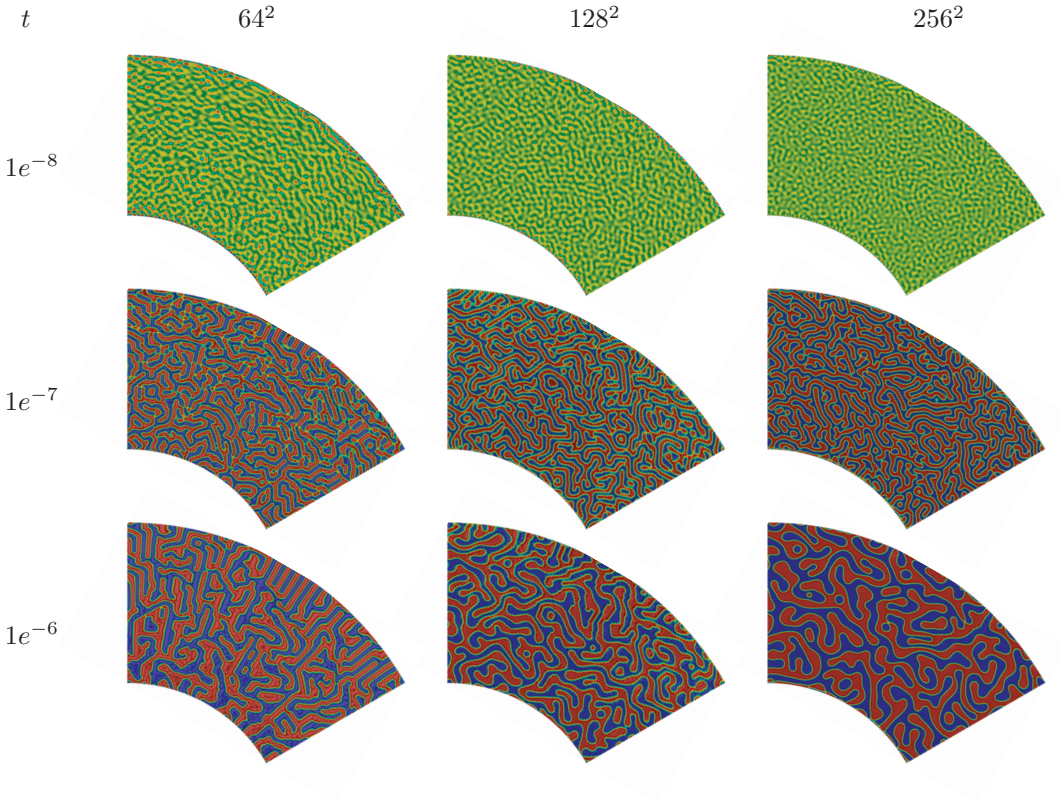

Figure 3: Phase-field separation. Evolution from the initial random distribution is shown at four time steps, for the three different meshes considered.

is also noticeable on the radial component of the velocity, where the highest values appears towards the outer wall. The high values close to the inner wall are dissipated.

The effect of the surface tension on the velocity field depends on the surface tension coefficient λ and the surface stress tensor. This tensor measures the curvature changes along the interface, and acts as a generation term in the momentum equation, producing a velocity in the opposite direction of the interface curvature changes. This effect coupled with the minimization of surface energy in the Cahn-Hilliard equation, results in a system that minimizes the interfacial energy faster than an advective Cahn-Hilliard system.

5 Conclusion

A novel discretization to solve the Navier-Stokes-Cahn-Hilliard equation was developed. It is implemented in PetIGA-MF, a multi-field high-performance implementation of divergence-conforming B-splines built on top of PetIGA. The discretization guarantees mass conservation for the problem through the use of these spaces. Spinodal decomposition under shear flow presents several time scales ruled by different phenomena. Our results show three main stages. The first one mainly shows phase separation, the second one seems to be governed by the

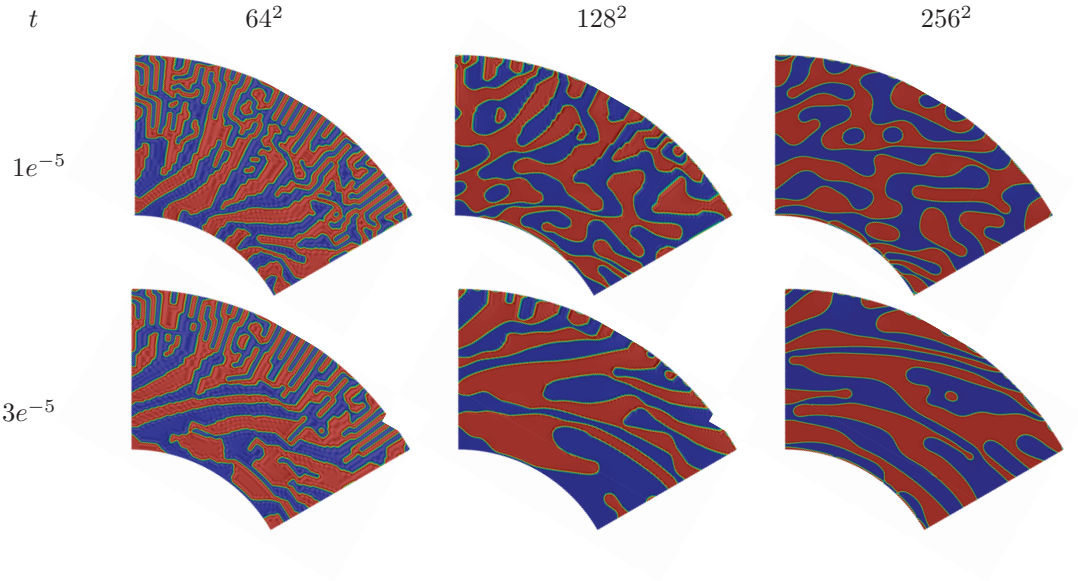

Figure 4: Phase-field evolution due to the velocity field at two different time steps. Results for the three different meshes considered are shown.

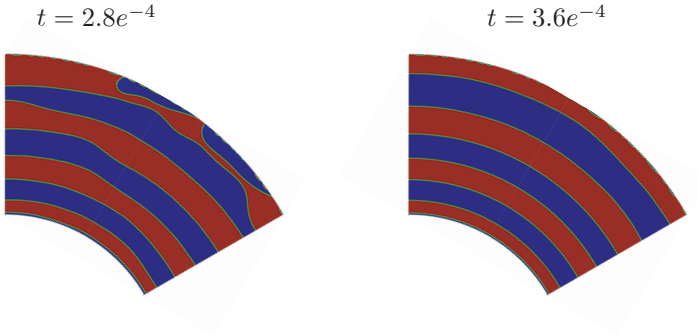

Figure 5: Formation of bands in the phase-field due to the velocity field in the mesh with 256^2-quadratic elements.

transport of the phases, while the last one is controlled by the characteristics of the flow. Including the surface stress term in the model is equivalent to including a source term in the momentum equation. This produces a new phenomenon that is not observed in the advective Cahn-Hilliard equation, which has an intrinsic time scale related to the interface morphology. From an energy-minimisation point-of-view, this term improves the dissipation properties of the system, and therefore can lead the system to reach the steady state faster.

6 Future work

The energy dissipation effect of the shear velocity and surface stress variations should be studied. This would improve the understanding behind the different phenomena taking place. The minimum resolution needed to solve the problem is also not clear: results differ for the three

different grids presented in this work. Even though results on minimum resolution needed to properly solve the Cahn-Hilliard equation as a function of the interfacial parameter γ are available [21], we intend to study convergence of the system by monitoring its total energy, which includes the kinetic energy coming form the Navier-Stokes equation and the free energy from the Cahn-Hilliard equation. Given the robustness PetIGA and PetIGA-MF have shown, it would seem that larger-scale simulations as well as three-dimensional results can be obtained.

References

[1] D. M. Anderson, G. B. McFadden, and A. A. Wheeler. Diffuse-interface methods in fluid mechanics. *Annual Review of Fluid Mechanics*, 30(1):139–165, 1998.

[2] G. K. Batchelor. *An Introduction to Fluid Dynamics*. Cambridge University Press, 2000.

[3] A. Buffa, C. de Falco, and G. Sangalli. IsoGeometric Analysis: Stable elements for the 2D Stokes equation. *International Journal for Numerical Methods in Fluids*, 65(11-12):1407–1422, 2011.

[4] A. Buffa, J. Rivas, G. Sangalli, and R. Vázquez. Isogeometric Discrete Differential Forms in Three Dimensions. *SIAM Journal on Numerical Analysis*, 49(2):818–844, 2011.

[5] A. Buffa, G. Sangalli, and R. Vázquez. Isogeometric analysis in electromagnetics: B-splines approximation. *Computer Methods in Applied Mechanics and Engineering*, 199(1720):1143 – 1152, 2010.

[6] J. W. Cahn and J. E. Hilliard. Free energy of a nonuniform system. i. Interfacial free energy. *J. Chem. Phys*, 28(258), 1958.

[7] J. W. Cahn and J. E. Hilliard. Free Energy of a Nonuniform System. iii. Nucleation in a Two-Component Incompressible Fluid. *J. Chem. Phys.*, 31(3):688–699, 1959.

[8] N. Collier, L. Dalcin, and V. M. Calo. PetIGA: High-performance isogeometric analysis. *arxiv*, (1305.4452), 2013. http://arxiv.org/abs/1305.4452.

[9] N. Collier, L. Dalcin, and V. M. Calo. On the computational efficiency of isogeometric methods. *International Journal for Numerical Methods in Engineering*, 100(8):620–632, 2014.

[10] N. Collier, L. Dalcin, D. Pardo, and V. M. Calo. The cost of continuity: performance of iterative solvers on isogeometric finite elements. *SIAM Journal on Scientific Computing*, 35(2):A767–A784, 2013.

[11] N. Collier, D. Pardo, L. Dalcin, M. Paszynski, and V. M. Calo. The cost of continuity: A study of the performance of isogeometric finite elements using direct solvers. *Computer Methods in Applied Mechanics and Engineering*, 213-216(0):353 – 361, 2012.

[12] A. M. A. Côrtes, A. L. G. A. Coutinho, L. Dalcin, and V. M. Calo. Performance evaluation of block-diagonal preconditioners for the divergence-conforming B-spline discretization of the Stokes system. *Journal of Computational Science*, (0):–, in press, 2015.

[13] A. M. A. Côrtes, P. Vignal, A. Sarmiento, D. García, N. Collier, L. Dalcin, and V. M. Calo. Solving nonlinear, high-order partial differential equations using a high-performance isogeometric analysis framework. In *CARLA, CCIS 485*, pages 236–247, 2014.

[14] J. A. Cottrell, T. J. R. Hughes, and Y. Bazilevs. *Isogeometric Analysis: Toward Unification of CAD and FEA*. John Wiley and Sons, 2009.

[15] L. Demkowicz. *Computing with hp-Adaptive Finite Elements, Vol. 1: One and Two Dimensional Elliptic and Maxwell Problems*. Chapman & Hall/CRC, 1st edition, 2006.

[16] D. Derks, D. G. A. L. Aarts, D. Bonn, and A. Imhof. Phase separating colloid polymer mixtures in shear flow. *Journal of Physics: Condensed Matter*, 20(40):404208, 2008.

[17] J. A. Evans, Y. Bazilevs, I. Babuška, and T. J. R. Hughes. n-widths, sup-infs, and optimality ratios for the k-version of the isogeometric finite element method. *Computer Methods in Applied Mechanics and Engineering*, 198(21-26):1726–1741, 2009.

[18] J. A. Evans and T. J. R. Hughes. Isogeometric divergence-conforming B-splines for the steady Navier-Stokes equations. *Mathematical Models and Methods in Applied Sciences*, 23(08):1421–1478, 2013.

[19] J. A. Evans and T. J. R. Hughes. Isogeometric divergence-conforming B-splines for the unsteady Navier-Stokes equations. *Journal of Computational Physics*, 241(0):141 – 167, 2013.

[20] X. Feng. Fully discrete finite element approximations of the Navier-Stokes-Cahn-Hilliard diffuse interface model for two-phase fluid f lows. *SIAM Journal on Numerical Analysis*, 44(3):pp. 1049–1072, 2006.

[21] H. Gómez, V. M. Calo, Y. Bazilevs, and T. J. R. Hughes. Isogeometric analysis of the Cahn-Hilliard phase-field model. *Computer Methods in Applied Mechanics and Engineering*, 197(49-50):4333–4352, 2008.

[22] H. Gómez and X. Nogueira. An unconditionally energy-stable method for the phase field crystal equation. *Computer Methods in Applied Mechanics and Engineering*, 249-252(0):52–61, 2012.

[23] T. Hashimoto, K. Matsuzaka, E. Moses, and A. Onuki. String phase in phase-separating fluids under shear flow. *Phys. Rev. Lett.*, 74:126–129, Jan 1995.

[24] T. J. R. Hughes. *The Finite Element Method: Linear Static and Dynamic Finite Element Analysis*. Dover, New York, 2000.

[25] T. Imaeda, A. Onuki, and K. Kawasaki. Anisotropic spinodal decomposition under shear flow. *Progress of Theoretical Physics*, 71(1):16–26, 1984.

[26] K. E. Jansen, C. H. Whiting, and G. M. Hulbert. A generalized-α method for integrating the filtered Navier-Stokes equations with a stabilized finite element method. *Computer Methods in Applied Mechanics and Engineering*, 190(3-4):305 – 319, 2000.

[27] R. LeVeque. *Finite Difference Methods for Ordinary and Partial Differential Equations: Steady-State and Time-Dependent Problems (Classics in Applied Mathematics Classics in Applied Mathemat)*. Society for Industrial and Applied Mathematics, Philadelphia, PA, USA, 2007.

[28] J. Liu, L. Dedè, J. A. Evans, M. J. Borden, and T. J. R. Hughes. Isogeometric analysis of the advective Cahn-Hilliard equation: Spinodal decomposition under shear flow. *Journal of Computational Physics*, 242(0):321 – 350, 2013.

[29] A. Onuki. Phase transitions of fluids in shear flow. *Journal of Physics: Condensed Matter*, 9(29):6119, 1997.

[30] N. Provatas and K. Elder. *Phase-Field Methods in Materials Science and Engineering*. Wiley-VCH, 1st edition, 2010.

[31] A. Sarmiento, A. M. A. Cortes, D. Garcia, L. Dalcin, N. Collier, and V. M. Calo. PetIGA-MF: a multi-field high-performance implementation of divergence-conforming B-splines. *Submitted*, 2014.

[32] O. Soriano-Vargas, E. O. Avila-Davila, V. M. Lopez-Hirata, N. Cayetano-Castro, and J. L. Gonzalez-Velazquez. Effect of spinodal decomposition on the mechanical behavior of Fe-Cr alloys. *Materials Science and Engineering: A*, 527(12):2910 – 2914, 2010.

[33] P. Vignal, L. Dalcin, D. L. Brown, N. Collier, and V. M. Calo. An energy-stable convex splitting for the phase-field crystal equation. submitted, 2014.

[34] P. A. Vignal, N. O. Collier, and V. M. Calo. Phase field modeling using PetIGA. In *Procedia Computer Science*, volume 18, pages 1614–1623, 2013.

[35] A. J. Wagner and J. M. Yeomans. Phase separation under shear in two-dimensional binary fluids. *Phys. Rev. E*, 59:4366–4373, Apr 1999.

[36] O. Wodo and B. Ganapathysubramanian. Computationally efficient solution to the Cahn-Hilliard equation: Adaptive implicit time schemes, mesh sensitivity analysis and the 3d isoperimetric problem. *Journal of Computational Physics*, 230(15):6037 – 6060, 2011.

[37] Y. Wu, H. Skrdla, T. Lookman, and S. Chen. Spinodal decomposition in binary fluids under shear flow. *Physica A: Statistical Mechanics and its Applications*, 239(13):428 – 436, 1997.